Wood-decay type and fungal guild dominance across a North American log transplant experiment

François Maillard, Michelle A Jusino, Erin Andrews, Molly Moran, Grace J Vaziri, Mark T Banik, Nicolas Fanin, Carl C Trettin, Daniel L Lindner, Jonathan S Schilling

Fungal Ecology 59 (2022) 101151

Contents lists available at ScienceDirect

Fungal Ecology

journal homepage: www.elsevier.com/locate/funeco

Wood-decay type and fungal guild dominance across a North American log transplant experiment

François Maillard [a,*], Michelle A. Jusino [b,c], Erin Andrews [a], Molly Moran [a], Grace J. Vaziri [b], Mark T. Banik [b], Nicolas Fanin [d], Carl C. Trettin [e], Daniel L. Lindner [b], Jonathan S. Schilling [a,**]

[a] Department of Plant & Microbial Biology, University of Minnesota, St. Paul, MN, USA
[b] Center for Forest Mycology Research, Northern Research Station, USDA Forest Service, Madison, WI, USA
[c] Department of Plant Pathology, University of Florida, Gainesville, FL, USA
[d] INRAE, UMR 1391 ISPA, Bordeaux Sciences Agro, Villenave d'Ornon, France
[e] Center for Forested Wetlands Research, USDA Forest Service, Cordesville, SC, USA

ARTICLE INFO

Corresponding Editor: Prof. L. Boddy

Keywords:
Wood rot fungi
Decay type
Soft rot
White rot
FACE
HTAS
Metabarcoding
Brown rot

ABSTRACT

We incubated 196 large-diameter aspen (*Populus tremuloides*), birch (*Betula papyrifera*), and pine (*Pinus taeda*) logs on the FACE Wood Decomposition Experiment encompassing eight climatically-distinct forest sites in the United States. We sampled dead wood from these large-diameter logs after 2 to 6 y of decomposition and determined wood rot type as a continuous variable using the lignin loss/density loss ratio (L/D) and assessed wood-rotting fungal guilds using high-throughput amplicon sequencing (HTAS) of the ITS-2 marker. We found L/D values in line with a white rot dominance in all three tree species, with pine having lower L/D values than aspen and birch. Based on HTAS data, white rot fungi were the most abundant and diverse wood-rotting fungal guild, and soft rot fungi were more abundant and diverse than brown rot fungi in logs with low L/D values. For aspen and birch logs, decay type was related to the wood density at sampling. For the pine logs, decay type was associated with the balance between white and brown/soft rot fungi abundance and OTU richness. Our results demonstrate that decay type is governed by biotic and abiotic factors, which vary by tree species.

1. Introduction

Dead wood represents an essential ecological niche for various macro- and microorganisms, sustaining forest biodiversity (Rayner and Boddy 1988; Harmon et al., 1986; Hoppe et al., 2016; Johnston et al., 2016; Skelton et al., 2019). From a biogeochemical perspective, dead wood is central to forest productivity and forest carbon (C) sequestration by storing large amounts of nutrients and C that are recycled or stabilized through the decomposition processes (Chambers et al., 2000; Baldrian and Lindahl 2011; Magnússon et al., 2016). However, dead wood not only represents an ecological and biogeochemical component of forests but is also considered by humans to be a resource for construction and energy production, notably through intensive forestry practices (Davidson and Janssens, 2006; Canadell and Raupach, 2008; Edenhofer et al., 2014). Collectively, this means that the fate of dead wood C is flexible and within some measure of human control in managed forests (Meinshausen et al., 2009; Thornton et al., 2014). Accurate predictions of wood decay rates and fates for C released by decomposers are critical, unmet challenges for Earth Systems modeling (Keenan et al., 2013).

The role of dead wood in the C cycle has historically benefited from important modeling efforts (Dai et al., 2021; Lustenhouwer et al., 2020). On a large scale, wood decay rates have been described as associated with temperature and precipitation (A'bear et al., 2014; Bradford et al., 2014; Harmon et al., 2020). Additionally, the position of dead wood (ground contact vs. aboveground) has been identified as a factor influencing decay rates, usually slower for dead wood standing vertically than for horizontal logs (Harmon et al., 2013; Russel et al., 2015). Wood's initial intrinsic characteristics, notably its density, carbon/-nitrogen ratio, extractives, and nutrient content affect decay rates (Weedon et al., 2009; Zanne et al., 2015; Harmon et al., 2020). However, dead wood presents unique specificities compared to other plant-derived organic matter types, such as leaf and microbial litter. During decomposition, physicochemical properties of leaf litter and

* Corresponding author.
** Corresponding author.
E-mail addresses: francois.maillard2@gmail.com (F. Maillard), schillin@umn.edu (J.S. Schilling).

https://doi.org/10.1016/j.funeco.2022.101151
Received 24 September 2021; Received in revised form 8 February 2022; Accepted 10 February 2022
Available online 7 March 2022

microbial biomass tend to converge, making C modeling mainly dependent on decay rates (Fierer et al., 2009; Preston et al., 2009; Wallenstein et al., 2013; Maillard et al., 2020; Ryan et al., 2020). Dead wood does not always exhibit this physicochemical convergence phenomenon. Indeed, substantial chemical divergences emerge through wood decomposition, generating very different decay types and potentially contrasting consequences for biogeochemical cycles (Keenan et al., 2013; Schilling et al., 2020). Although wood decay rates have profited C modeling efforts, the fates for carbon reallocated to soils or atmosphere as a function of wood decay types have been poorly investigated and need attention.

In temperate and boreal forests, fungal communities have been characterized as the primary agents of wood decomposition (Rayner and Boddy 1988; Lindner et al., 2011; van der Wal et al., 2014). These fungal decomposers are responsible for the different decay types observed in dead wood (Schilling et al., 2020). Decay nutritional modes, also known as decay or rot types, have been proposed as functional traits for regrouping different fungal lineages within functional guilds (Blanchette 1980). With the capacity to synthesize peroxidases and glycosyl hydrolase enzymes, white rot (WR) fungi cause substantial removal of lignin and carbohydrates during wood decomposition (Eriksson et al., 1990; Zhang et al., 2019). Conversely, brown rot (BR) fungi access and decompose carbohydrates using Fenton-based chemistry, with only minor removal of lignin (Riley et al., 2014; Schilling et al., 2020). The soft rot (SR) fungi, less studied than the two other wood-rotting types, have been described as using wood cell wall erosion to access carbohydrates, with low lignin removal similar to brown rot fungi (Eslyn et al., 1975; Nilsson et al., 1989; Blanchette et al., 2010). With contrasting wood decomposition mechanisms, these three wood-rotting fungal guilds (BR, SR, and WR) may drive major differences in the forest C cycle. BR and SR fungi, in particular, might increase forest soil C stocks by generating recalcitrant particulate lignin (Stutz et al., 2017). In contrast, by mineralizing lignin, WR fungi might limit the contribution of wood to stable soil organic matter formation. The fate of lignin decomposed by WR fungi is still uncertain and depends on two phenomena: (1) the polyphenols resulting from lignin depolymerization might adsorb on mineral particles and create stable mineral-associated organic matter (Stutz et al., 2019); or (2) lignin might be completely mineralized by WR fungi, limiting lignin-associated C transfer and stabilization in soil (Del Cerro et al., 2021).

Decay-type assessment presents a technical challenge. Scanning electron microscopy has been defined as one of the most accurate approaches to identifying different rot types (Riley et al., 2014). However, while useful for laboratory experiments using dead wood decomposed by a single fungal species, scanning electron microscopy is challenging to scale up to the field, where multiple wood-rotting fungi decompose the same wood logs in parallel or successively. For this purpose, chemical approaches were developed, and notably, the continuous variable (not binary brown vs. white rot type) ratio of lignin loss (L) to density loss (D) (Worrall et al., 1997; Schilling et al., 2015, 2020). By extending the results of Worrall et al. (1997), Schilling et al. (2020) found that wood decomposed by WR fungi have a high L/D, usually ranging from 5 to 0.8 and decreasing with decomposition time, which is caused by progressive removal of lignin. Conversely, BR and SR fungi were characterized by L/D ratios below 0.8, being relatively stable during the decomposition time, due to the selective extraction of the carbohydrates. Still, despite the emergence of this robust tool to categorize dead wood physicochemical properties, the study of the decay type prevalence in the field remains primarily indirectly explored by assessing the wood-rotting fungal guilds abundance.

Sporocarp investigations of wood-rotting fungi across North American forests revealed that latitude affects BR and WR fungal distributions, which dominate higher and lower latitudes, respectively (Gilbertson 1980). However, SR fungal distributions have been poorly studied; SR fungi are often described as stress-tolerant fungi that inhabit extreme environments, such as polar regions, deserts, or wet tropical forests (Blanchette et al., 2010). The different latitudinal distributions between BR and WR fungi may result from climatic parameters (temperature and/or precipitation), with BR fungi preferring colder and drier habitats and WR fungi favoring warmer and wetter environments (Gilbertson 1980). Host tree phylogeny, notably gymnosperms, which are usually more abundant at higher latitudes, might also explain the distribution of BR and WR fungi (Gilbertson 1980). In contrast to WR fungi, Gilbertson (1980) notably found that BR fungi were strongly associated with gymnosperm tree species. Recently, an evolutionary study challenged current thoughts about the angiosperm/gymnosperm preferences of BR and WR fungi (Krah et al., 2018). Dead wood position (horizontal on the ground or standing vertically) has also been described as affecting wood-rotting guild distribution, with BR species being more abundant in logs lacking contact with soil, while WR fungi were more abundant in dead wood that is in direct contact with the forest floor (Jaroszewicz et al., 2021). Finally, decomposition time is also an important factor explaining wood-rotting fungal dominance. BR fungi have been observed to be relatively abundant at the beginning of the decomposition process, and WR fungi to be relatively stable throughout wood decomposition (Rajala et al., 2012, 2015; Fukasawa et al., 2019). Few, if any studies have investigated the biotic and abiotic drivers of wood-rotting fungal guild balance using high-throughput amplicon sequencing (HTAS) technologies (WR, BR, and SR relative abundances and ratios) and their impacts on dead wood decay types.

This study assessed wood decay types and the wood-rotting fungal guilds of three tree species (two angiosperms, aspen (*Populus tremuloides*) and birch (*Betula papyrifera*), and one gymnosperm, loblolly pine (*Pinus taeda*)) at eight distinct forest sites across North America (Fig. 1). Tree boles (logs) were left to decompose for up to 6 y and sampled after 2, 4 or 6 y depending on site decay rates and log species. For the pine species, we included a log ground contact/orientation treatment comparing boles that were decomposing horizontally on the forest floor and boles that were standing vertically without ground contact. Dead wood was sampled to assess wood-rotting fungi relative abundance and OTU richness (using DNA metabarcoding and sequencing of the ITS2 fungal marker) and wood physicochemistry (final wood density and L/D ratio). Fungal operational taxonomic units (OTUs) were classified as BR, SR, or WR decay types using databases and literature resources. Decay rates (wood density at sampling), wood decay type (L/D ratio), and wood-rotting fungal guilds were linked with climate parameters (mean annual precipitation [MAP] and mean annual temperature [MAT]) using structural equation modeling. Based on the physiologies and ecologies of the different wood-rotting fungal guilds, we tested the following predictions: (P1) WR fungi will dominate aspen and birch dead wood, and pine dead wood will be rich in BR fungi as compared to aspen and birch; (P2) BR fungi will dominate northern, colder, sites while WR fungi will dominate southern, warmer, forests; (P3) Pine will have a lower-than-average L/D ratio due to more abundant BR fungi; and (P4) Vertically standing pine wood logs will be rich in BR fungi as compared to horizontal pine logs and will also have a lower L/D ratio.

2. Materials and methods

2.1. Experimental design

This study utilizes samples from the decommissioned U.S. Dept. of Energy's Free Air Carbon Dioxide Enrichment (FACE) Wood Decomposition Experiment (FWDE). The FWDE (Trettin et al., 2021) is designed to assess wood decomposition and the fate of the associated wood-carbon across major forested biogeoclimatic zones across the continental United States. We retained eight among the nine study sites of the FWDE (Table 1, Fig. 1). These Experimental Forest sites have annual precipitation means that range from 58.9 cm at a site in Colorado to 228.1 cm at a site in North Carolina. Mean annual temperatures range from 4.2 °C in Montana to 18.8 °C in South Carolina.

The FWDE utilized elevated and control logs obtained from the FACE

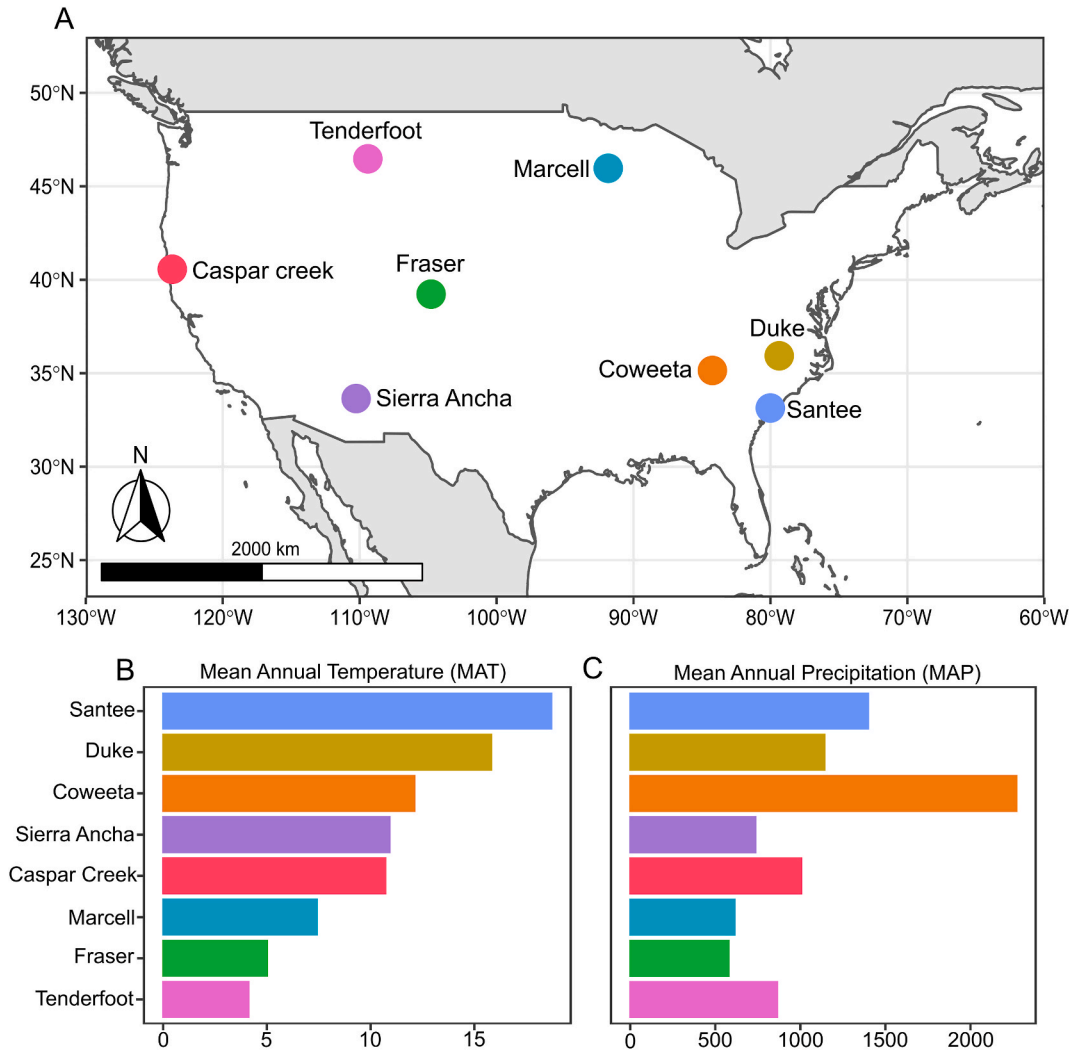

Fig. 1. Location of the experimental sites.

Table 1
Locations and descriptions of FACE experimental sites.

Site	Code	State	Latitude (°N)	Longitude (°W)	Altitude (m)	Forest Type
Caspar Creek	CC	CA	39.3726	123.7063	240	Douglas-fir
Coweeta	CO	NC	35.0467	83.4574	910	Oak-hickory
Duke	DU	NC	33.9760	79.0924	170	Loblolly-shortleaf pine
Fraser	FR	CO	39.9296	105.8698	2710	Fir-spruce
Marcell	MA	MN	47.5057	93.4861	430	White-red-jack pine
Santee	SA	SC	33.1482	79.7910	8	Loblolly-shortleaf pine
Sierra Ancha	SI	AZ	33.8039	110.9159	2220	Ponderosa pine
Tenderfoot	TE	MT	46.9236	110.8697	2130	Lodgepole pine

experiment; pine logs were obtained from the Duke Forest in North Carolina and the aspen and birch logs were obtained from the Rhinelander, Wisconsin site. The aspen and birch logs were cut into 1 m long sections (pine into 2 m sections) and 24 of each were placed horizontally on the ground. An additional 24 pine logs were placed vertically atop PVC pipe stands and wired into place as an above ground, vertical treatment. The material was deployed in 2011; for details on the experimental design, set-up and characteristics of the sites, see Trettin et al. (2021).

2.2. Sampling and wood property analyses

For an L/D assessment to correctly determine rot type, there must be some decay (higher than decay class 1) but not so much decay loss that density and content chemistries are no longer distinguishable as wood versus soil (typically, lower than decay class 4) (Schilling et al., 2015). To target decay classes 2 and 3, we sampled wood after 2, 4 or 6 y of decomposition depending on the log species and experimental site, when the wood had not surpassed decay class 3 and only in samples that had progressed above decay class 1 (Table S1). Both dead wood originating from control and carbon dioxide enrichment FACE treatments were sampled and regrouped as a unique treatment in our study. A 3-cm disk was cut from log ends for DNA extractions (described below), with a second adjacent disk cut for oven-drying and lignin analysis (gravimetrically, as acid-insoluble lignin in 72% H_2SO_4). Densities were also calculated (dry weight (g) per fresh volume (cm^3)) by weighing whole

logs, in the field, and drying material from disk 2 to measure and adjust for moisture content. Using these measures, and as outlined in Schilling et al. (2015), we calculated the loss of lignin relative to the loss of density (L/D) to create a continuous variable as a carbohydrate selectivity index, with lignin-degrading white rot having reliable L/D > 0.8 (Schilling et al., 2020). Given that there can be more progressive decay near the log ends with exposed grain, it is useful to note that densities were calculated based on whole-log measurements rather than on samples from these disks, and that the lignin analysis from the inner disk was adjusted to a 'store' (content per volume rather than per mass) by using these whole-log densities.

2.3. Fungal community sequencing

For DNA extraction, samples were collected after 2 or 6 y of decomposition depending on the log species and experimental site by drilling three holes per log and collecting the resulting drill shavings (Table S1). Each horizontal log was sampled for DNA approximately 10 cm from the end by drilling three 3.175 mm diameter holes (approximately 3 cm deep) at approximately 0, 90 and 270 °, with zero being the top of the log. Vertical logs were sampled at 3 points, which were randomly selected from 4 cardinal points (0, 90, 180 or 270). Holes were drilled similar to the methods of Jusino et al. (2020). Drill bits were washed and DNA-sterilized between each use following Jusino et al. (2020). After collection, drill shavings were covered with a buffered 2% CTAB cell lysis buffer solution (CLS; Lindner and Banik, 2011) and frozen at −20 °C. The DNA was subsequently extracted from the samples following the protocol of Lindner and Banik (2011). The first step of the extraction involves a 2-h incubation at 65C, following this incubation, the three samples from each log were pooled for the remainder of the extraction. Negative controls (CLS with no sample) were included during every batch of DNA extraction to control for possible contamination at the DNA extraction step.

After extraction we PCR amplified the fungal DNA for HTAS libraries using individually barcoded Ion fungal-specific primers fITS7 and ITS4 (Ihrmark et al., 2012) that were modified to be compatible for Ion Torrent sequencing (Ihrmark et al., 2012) according to manufacturer's recommendations. The forward primer consisted of the Ion A adapter sequence, the Ion key signal sequence, a unique Ion Xpress Barcode sequence (10–12 bp), a single base-pair linker (A), and finally the fITS7 primer (Ihrmark et al., 2012). The reverse primer consisted of the Ion trP1 adapter sequence followed by the conserved ITS4 primer (Ihrmark et al., 2012). The following reagents were used for each PCR reaction: 7.88 μl DNA-free molecular grade water, 3.0 μl Green GoTaq 5x buffer (Promega Corporation, Madison, WI, USA) – final concentration 1x, 0.3 μl of 10 mM dNTPs (Promega Corporation, Madison, WI, USA) for a final concentration 0.2 mM of each dNTP, 0.3 μl of each 10 μM primer for a final concentration of 0.2 μM of each primer, 0.12 μl of 20 mg/ml BSA (New England BioLabs), 0.1 μL of 5u/μL GoTaq polymerase (Promega) – final concentration of 0.033 u/μL of the reaction, and 3.0 μL of template DNA for a total reaction volume of 15 μL. Each PCR cycle was run with a negative control (same reagents, substituting water DNA-free molecular grade water for the full volume of template DNA). Thermocycling conditions were: initial denaturation of 94 °C for 3 min, then 11 cycles of (94 °C for 30 s, 60 °C for 30 s (drop 0.5 °C per cycle), 68 °C for 1 min), then 26 cycles of (94 °C for 30 s, 55 °C for 30 s, and 68 °C for 1 min), with a final extension of 68 °C for 7 min. An additional sample consisting of SynMo (Palmer et al., 2018), an equimolar spiked-in mock community control composed of non-biological synthetic ITS sequences, was also amplified and included in each sequencing run. PCR products, including negative extraction controls, and negative PCR controls were visualized on agarose gel, to confirm amplification of the target region, and rule out possible contamination during extraction or PCR steps. Zymo Select-a-size spin columns were used to purify the PCR products (Zymo Research, Irvine, CA, USA). After purification, libraries were quantified using a Qubit® 2.0 Fluorometer with the high-sensitivity DNA quantification kit (ThermoFisher Scientific, Madison, WI, USA), equilibrated and then combined to form sequencing libraries. The barcoded libraries were sequenced on the Ion Torrent semiconductor sequencing platform. Raw sequence data were deposited in the NCBI SRA under PRJNA779094.

2.4. Bioinformatics

We processed our Ion Torrent data using AMPtk version 1.4.0 (Palmer et al., 2018; amptk.readthedocs.io). Each run was pre-processed separately, then concatenated prior to clustering. We pre-processed our merged, individually barcoded reads using USEARCH (version 9.2.64), vsearch (version 2.9.0) and then removed the forward and reverse ITS primers. We discarded any reads shorter than 125 bp. Reads longer than 300 bp were trimmed to 300 and any reads shorter than 300 bp were padded with Ns to help improve the clustering step (Palmer et al., 2018). Sequence reads were then quality-filtered with expected errors less than 1.0 (Edgar and Flyvbjerg 2015), de-replicated, and clustered at 97% similarity to generate operational taxonomic units (OTUs) using UPARSE (Edgar 2013). Following clustering, any padded Ns were removed, and the processed sequences were mapped to the OTUs. We used SynMo (Palmer et al., 2018) to account for observed rates of barcode crossover using the filter module in AMPtk. Following filtering, the LULU script (version 0.1.0; Frøslev et al., 2017) was used for further post-clustering curation. Taxonomic assignment of the OTUs was achieved using the hybrid taxonomy algorithm in AMPtk. All non-fungal OTUs were removed following taxonomy assignment.

2.5. Data analyses

Data analyses and visualizations were performed using R software version 4.0.5 (R Core Team, 2021). To account for variations in total sequence read counts across samples, all fungal community analyses were based on counts rarefied to 10,072/sample (see Fig. S1 for the rarefaction curves) in the vegan package (Oksanen et al., 2013). The 196 samples had a total of 1,974,112 sequences and 3334 fungal OTUs present in the final quality-controlled and rarefied dataset. Based on the assigned taxonomy, fungal OTUs were classified as BR, SR, or WR fungi using a combination of different databases and literature resources (Levy 1969; Nilsson 1973; Bugos et al., 1988; Zabel et al., 1991; Worrall et al., 1997; KarunasekeraDaniel, 2015; Nguyen et al., 2016; Pedersen et al., 2020; Põlme et al., 2020; Fukasawa and Matsukura 2021). Rot types superseded trophic status, so for example, plant pathogenic fungi presenting as an SR type were classified as SR fungi. The detailed list of classified taxa is provided in Table S2. The WR, BR and SR relative abundances and OTU richness were then calculated and used as quantitative metrics of dead wood colonization by the different wood-rotting fungal guilds. Samples presenting wood decay type (L/D ratio) values below 0.8 were classified as presenting SR/BR decay, and values over 0.8 were classified as WR decay (Worrall et al., 1997; Schilling et al., 2015, 2020). The L/D ratio was then used as a continuous variable for the statistical analyses. Additionally, wood density at sampling was considered as an indicator of decomposition rate, with low density indicating an advanced decay stage as described in Rajala et al. (2015).

The effects of tree species (aspen, birch, or pine) on the L/D ratio and the relative abundance and OTU richness of BR, SR, and WR fungi were evaluated for horizontal log positions, and depending on the log position using the Kruskal–Wallis test by ranks followed by a post hoc test using the criterion Fisher's least significant difference ($P \leq 0.05$) given that assumption of homoscedasticity was not respect nor improved after normalization. Samplings were conducted independently and without perfect coordination for wood chemistry analysis and fungal community sequencing, leading to a limited number of logs presenting both L/D and wood-rotting guilds information. Consequently, given this imbalanced experimental design and the lack of replicates at some study sites, tree species effects on the L/D ratio and the relative abundance of BR, SR,

and WR for horizontal log positions were tested only for Caspar Creek (CC), Fraser (FR), Marcell (MA), Santee (SA), Sierra Ancha (SI), and Tenderfoot (TE) sites. For similar reasons, log position effects on the L/D ratio and BR, SR, and WR relative abundance for pine tree species were tested only for Caspar Creek (CC), Coweeta (CO), Duke (DU), Marcell (MA), Santee (SA), and Tenderfoot (TE) sites. The site effect was measured by L/D, final wood density, and BR, SR, and WR relative abundance using the Kruskal–Wallis test by ranks ($P \leq 0.05$) (Figs. S2, S3, S4, S5 and S6). Because L/D results from the decomposition history of dead wood, likely including different types of wood-rotting fungi, we used ratios between the relative abundance and the OTU richness of the different wood-rotting fungal guilds. Based on the literature, we expected WR fungi to have an increased L/D compared to BR and SR fungi (Schilling et al., 2015, 2020). Thus, we calculated the WR/BR, WR/SR, and WR/(BR + SR) ratios.

We tested for relationships between L/D and wood rot fungi ratios using Pearson's correlation ($P \leq 0.05$) for the different combinations of three species and log orientations (horizontal aspen, birch, and pine, and vertical pine). We applied structural equation modeling (SEM) based on an a priori model (Fig. S2) to elucidate the direct and indirect effects of climate (MAP and MAT), decay stage (final wood density), and wood-rotting fungi ratios on L/D. Final wood density (referred to as density in the graphs) was used as a proxy for the decay stage (Zalamea et al., 2007; Mäkipää and Linkosalo 2011; Chambers et al., 2000). SEM was performed using the lavaan package in R software (Rosseel, 2012). Wood density, MAP, and MAT variables were rescaled to limit variance inflation before SEM. Maximum likelihood estimation (MLM) was used as the estimator to account for the lack of normality of some variables. Wood-rotting fungi abundance and richness ratios were alternatively tested against the a priori model. The models presenting the best fit were kept for each combination of tree species and log orientation (horizontal aspen, birch, and pine, and vertical pine). The four models were then reduced to the best-fit models ($X^2 > 0.05$, RMSEA ≤ 0.08). The non-significant paths ($P > 0.05$) that improved model fit were kept in the final models.

3. Results

3.1. Tree species effect on wood decay type

When all sites were considered together for the horizontal log position, we found a large range of carbohydrate selectivity values ranging from 0 to 2.91 despite logs being transplanted from a common source. Most log L/D values reflected WR-dominated decay histories (>0.8). All birch samples had L/D > 0.8, and nearly 80 % of the aspen and pine (78.6 % and 78.3 % of logs tested, respectively) reflected a process more dominated by lignin-degrading WR fungi (Fig. 2). The L/D < 0.8 indicative of dominance of BR/SR decay processes was not recorded in birch, and was 21.4 % and 21.7 % for aspen and pine, respectively. Considered as a continuous variable, the average L/D was significantly ($P \leq 0.05$) lower for the pine (1.05) by comparison with aspen (1.24) and birch (1.40), indicating that pine decay had a higher carbohydrate selectivity than the angiosperms tested but was still a white rot-dominated process. The amount of L/D variation (standard deviation) was higher for the aspen (±0.58) than for the birch (±0.46) and pine (±0.32).

3.2. Wood log orientation effect on wood decay type

When all sites were considered together for the pine samples, decay type frequency was very similar between horizontally and vertically incubated wood logs and dominated by the WR decay type (86.8% and 89.8%, respectively) (Fig. 2). Wood log orientation did not significantly affect ($P > 0.05$) the L/D range (horizontal = 1.10, vertical = 1.19). L/D variation between pine samples incubated horizontally and vertically was also very similar (±0.30 and ± 0.34, respectively).

3.3. Tree species and log orientation effects on wood-rotting fungal guilds relative abundance and richness

Tree species identity significantly affected ($P \leq 0.05$) the relative abundance (Fig. 3) and the OTU richness (Fig. S3) of the three types of wood-rotting fungi. WR fungi relative abundance and OTU richness ($P \leq 0.05$) were significantly higher for the pine (abundance = 40.1 %; richness = 2.7 OTUs) by comparison with aspen (abundance = 26.4 %; richness = 1.6 OTUs) (Fig. 3A, and Fig. S3A). WR fungi relative abundance and OTU richness for the birch samples (abundance = 27.4 %; richness = 1.8 OTUs) were not significantly different from aspen and pine. SR fungi relative abundance and OTU richness were significantly higher ($P \leq 0.05$) in aspen (abundance = 25.8%; richness = 6 OTUs) and birch (abundance = 23.7 %; richness = 6.2 OTUs) samples than for pine (abundance = 6.8 %; richness = 3.7 OTUs) (Fig. 3B; Fig. S3B). BR fungi were relatively poorly abundant and diverse by comparison with WR and SR fungi and represented around ~2–3 % of the sequences and 0.6 OTU on average for the three studied tree species, being significantly ($P \leq 0.05$) more abundant and diverse in pine by comparison with aspen

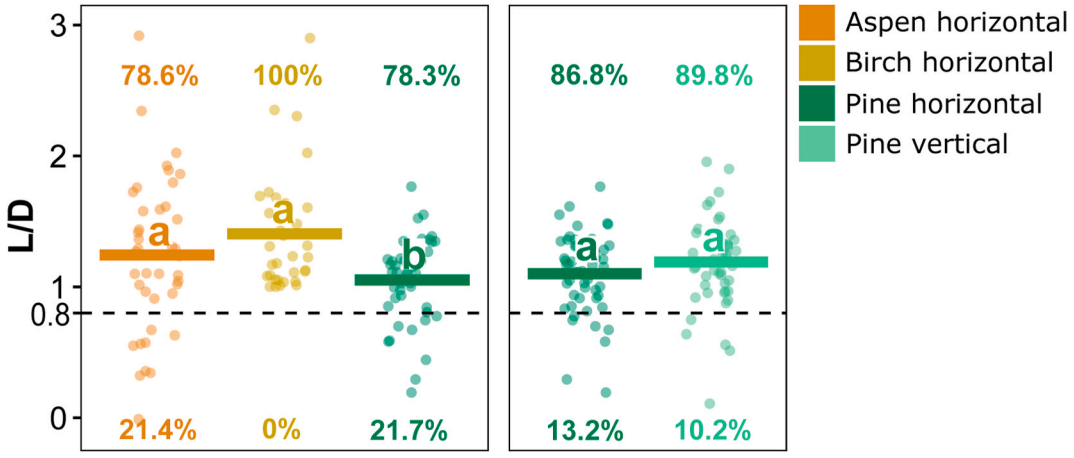

Fig. 2. L/D for the horizontal logs depends on the tree species (aspen, birch and pine for CC, FR, MA, SA, SI, and TE sites) and the log orientation for the pine (horizontal and vertical for CC, CO, DU, MA, SA, and TE sites). Horizontal bars represent the L/D average for all the sites together. The horizontal dashed bar at 0.8 L/D represents the threshold separating brown/soft rot and white rot decay types. L/D was compared using Kruskal–Wallis test by ranks. Different letters indicate significant differences (Fisher's Exact Test, $P \leq 0.05$). (For interpretation of the references to color in this figure legend, the reader is referred to the Web version of this article.)

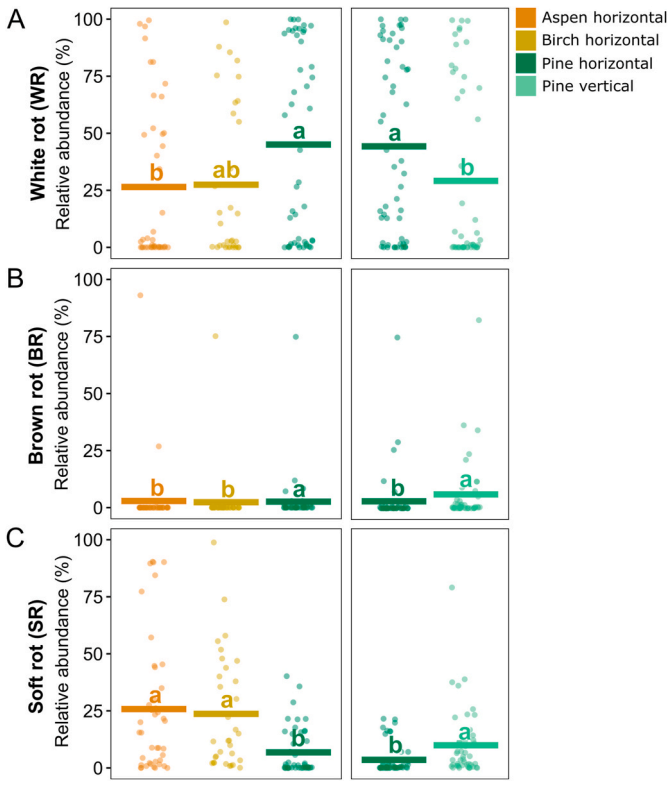

Fig. 3. (A) White (WR), (B) brown (BR), and (C) soft (SR) rot fungi relative abundance (%) for the horizontal logs depending on the tree species (aspen, birch and pine for CC, FR, MA, SA, SI, and TE sites) and depending on the log orientation for the pine species (horizontal and vertical for CC, CO, DU, MA, SA, and TE sites). Horizontal bars represent the L/D average for all sites together. WR, BR, and SR relative abundances were compared using Kruskal–Wallis test by ranks. Different letters indicate significant differences (Fisher's Exact Test, $P \leq 0.05$). (For interpretation of the references to color in this figure legend, the reader is referred to the Web version of this article.)

and birch (Fig. 3C; Fig. S3C).

Although wood log orientation had no significant effect on L/D for the pine species, it significantly affected ($P \leq 0.05$) the relative abundance and OTU richness of the three types of wood rot fungi (Fig. 3; Fig. S3). WR fungi were significantly less abundant and diverse in vertical pine samples (abundance = 29.1 %; richness = 1.2 OTUs) by comparison with the pine logs incubated horizontally (abundance = 44.3 %; richness = 3.1 OTUs) ($P \leq 0.05$) (Fig. 3A; Fig. S3A). On the contrary, BR and SR fungi were respectively significantly 99 % and 181 % more abundant and 196 % and 54 % more diverse in vertically incubated wood logs compared with the horizontal samples ($P \leq 0.05$) (Fig. 3B and C; Figs. S3B and S3C).

3.4. Relationships between climate, wood rot fungi and wood decay type

The site effect was examined using climate parameters (MAP and MAT). Differences in the final wood density, L/D, BR, SR and WR relative abundance and OTU richness depending on the site are available in the supplementary materials section (Figs. S1–S12). Relationships between wood-rotting fungi abundance and richness ratios and L/D were directly evaluated using Pearson's correlations. Due to the very low abundance and richness of the BR fungi for the aspen and birch, only the WR/SR ratio was considered for these two species. No significant correlations were found between L/D and WR/SR abundance and richness ratios for the aspen and birch tree species ($P > 0.05$) (Fig. 4A and B; Figs. S4A and S4B). Concerning horizontal and vertical pine samples, WR/BR, WR/SR and WR/(SR + BR) ratios were tested for their potential correlation with L/D. For the horizontal pine samples, L/D and relative abundance and OTU richness WR/(SR + BR) ratios were significantly positively correlated (abundance: $r = 0.32$, $P = 0.007$; richness: $r = 0.32$, $P = 0.009$) (Fig. 4C; Fig. S4C). When tested separately, WR/BR and WR/SR OTU richness but not relative abundance ratios were significantly correlated with the L/D for the pine samples incubated horizontally (WR/BR: $r = 0.32$, $P = 0.009$; WR/SR: $r = 0.29$, $P = 0.0195$). Pine vertical L/D was only significantly positively correlated with the WR/BR relative abundance ratio ($r = 0.41$, $P = 0.003$) (Fig. 4D; Fig. S4D), but significantly with the three OTU richness ratios (WR/BR: $r = 0.34$, $P = 0.0174$; WR/SR: $r = 0.29$, $P = 0.0435$; WR/(BR + SR): $r = 0.35$, $P = 0.0127$).

Each of the four selected models using ratios between wood-rotting guild relative abundance ratios had a good fit (Fig. 5). For the wood rot fungi abundance-based models, MAT was an important factor in explaining the final wood density for most of the treatments being significant for the birch (Fig. 5B), pine horizontal (Fig. 5C) and vertical (Fig. 5D) ($P \leq 0.05$) and as a trend for the aspen (Fig. 5A) ($P \leq 0.1$). For the vertical pine treatment, final wood density was also significantly explained by the MAP, which was not the case for the three horizontal treatments. WR/SR was not significantly associated with L/D for the aspen and birch species. The final wood density significantly explained L/D for the aspen and birch treatments. On the contrary, L/D was not explained by the final wood density but by the wood-rotting fungi ratios for the pine horizontal and vertical treatments. Final wood density had a relatively high level of explained variance for the pine vertical ($R^2 = 0.47$), pine horizontal ($R^2 = 0.33$) and birch ($R^2 = 0.24$) by opposition with the aspen ($R^2 = 0.05$). L/D variance explained based on our models was the best for the birch ($R^2 = 0.53$) followed by the pine vertical ($R^2 = 0.15$), pine horizontal ($R^2 = 0.11$), and aspen ($R^2 = 0.08$). The four selected models using ratios between wood-rotting guild richness ratios also had a good fit (Fig. S13). They provided very similar results to the relative abundance models regarding the factors significantly associated with density and L/D variance explanation. However, we noticed major differences between the abundance- and richness-based models concerning the prediction of the wood-rotting guild ratios. Explained variance for the wood-rotting fungi relative abundance ratios were much higher for the richness-based models (aspen: $R^2 = 0.39$; birch: $R^2 = 0.31$; horizontal pine: $R^2 = 0.23$) by comparison with the abundance-based models (aspen: $R^2 = 0.23$; birch: $R^2 = 0.17$; horizontal pine: $R^2 = 0.04$) for the horizontal logs. Wood-rotting guild ratio variance remained largely unexplained for the vertical pine logs (abundance: $R^2 = 0.08$; richness: $R^2 = 0.02$). For the abundance-based models, WR/SR ratios significantly positively correlated with MAT, while they significantly positively correlated with MAP for the richness-based models. Wood density at sampling was significantly negatively correlated with the richness WR/SR and WR/(BR/SR) ratios for the aspen and horizontal pine samples.

4. Discussion

In partial agreement with our prediction (P1), white rot dominated decomposition in wood and WR fungi dominated the fungi present in fungal communities for the three studied tree species. This included the wood of the conifer species, pine, despite commonly reported association of brown rot with conifer wood. This may reflect a general distinction in BR fungal prevalence between boreal and temperate forests. For example, Renvall (1995) reported that in Finnish boreal forests, 40%–50% of sporocarps found on *Pinus sylvestris* and *Picea abies* dead wood were BR fungi. These results were confirmed by amplicon sequencing studies, and BR fungi were identified as being equally as abundant as WR fungi during *Picea abies* wood decomposition in boreal forests (Rajala et al., 2015). In temperate forests, studies using sporocarp counting and fungal metabarcoding show generally fewer BR fungi. In German temperate forests, BR fungi sporocarps accounted for a relatively small proportion of the total fruit bodies in comparison to WR

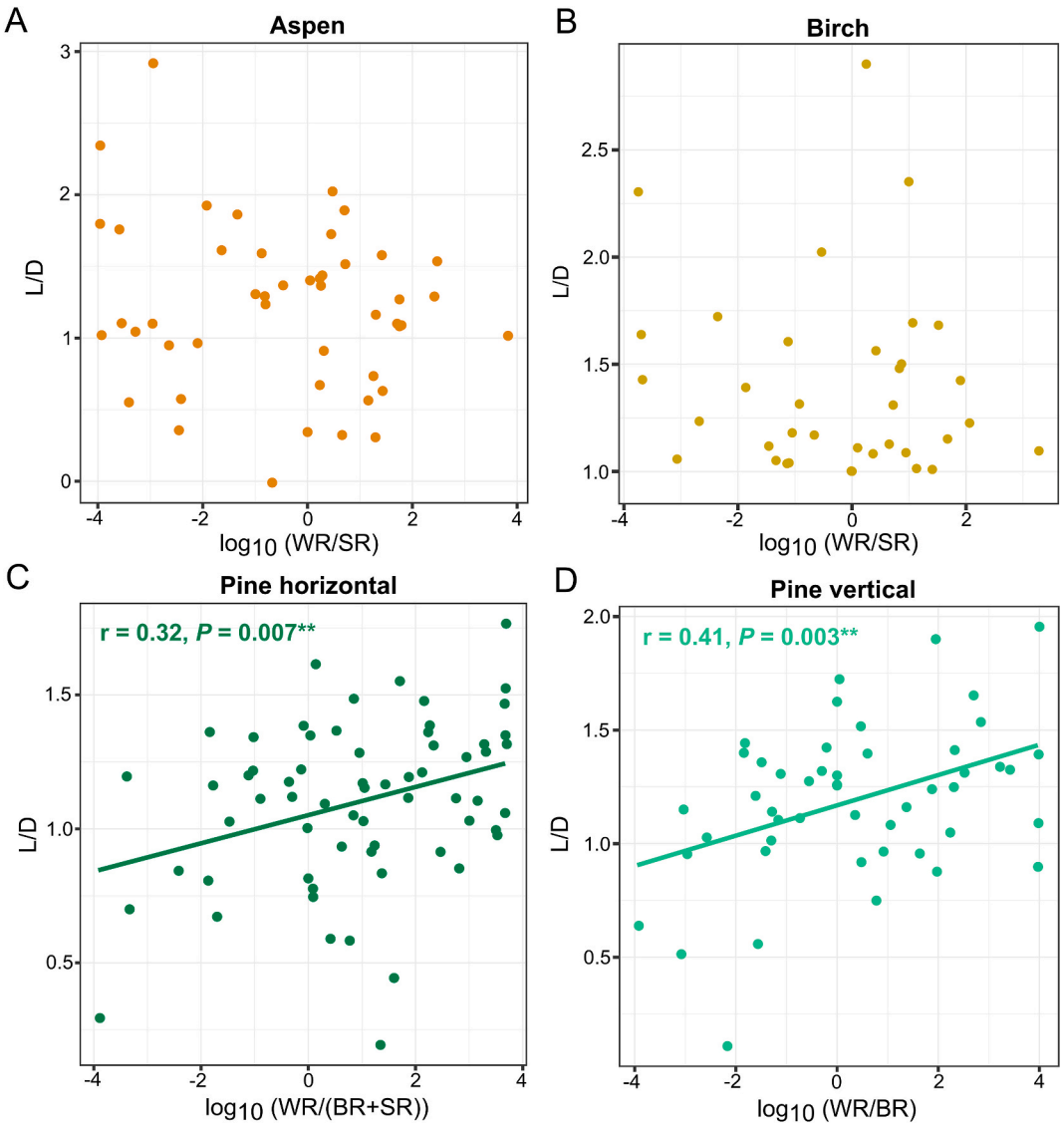

Fig. 4. Pearson's correlations between L/D and log10 ratio of the different rot type relative abundances with all the study sites regrouped together for (A) aspen, (B) birch, (C) horizontal pine, and (D) vertical pine dead wood. Only significant correlations are shown ($P \leq 0.05$).

fungi (Arnstadt et al., 2016). In the same study, BR fruit bodies were more frequently found colonizing *Pinus sylvestris* and *Picea abies* than *Fagus sylvatica* dead wood (Arnstadt et al., 2016). Leonhardt et al. (2019) explored the mycobiome of 13 angiosperm and gymnosperm tree species in temperate forests and highlighted that BR fungi rarely exceeded 5% of relative abundance, except for *Picea abies* (20%–25%), while WR fungi represented 30%–60% of the sequences. Similar results were found by Baldrian et al. (2016), with BR fungi being almost absent on *Fagus sylvatica* and *Abies alba* dead wood and representing only 15% of the sequences for *Picea abies*. Again, in temperate forests, Cline et al. (2018), Fukasawa and Matsuoka (2015a) and Viotti et al. (2021)each reported minor proportions of BR fungi in comparison to WR fungi in birch, pine, and oak dead wood. While relative abundance is often used as a metric of wood-rotting dominance in the recent literature, our results also showed that OTU richness depicted the same patterns. Taken together, these pieces of evidence parallel our results and point to a wood-rotting fungal balance being dominated by WR fungi in temperate forests.

This generalization does not undermine the importance of BR or SR in shaping global carbon emissions from wood. First, BR fungi in ITS datasets in Japan were recently shown not to align well with visual qualifications of BR in wood (Fukasawa 2015a; 2015b; Fukasawa and Matsukura 2021). In addition, there is an obvious caveat when linking a community snapshot of DNA and physiochemical consequences in wood, in that a snapshot may not adequately describe the entire decomposition process. Second, shifts in the balance between rot types may be more consequential and susceptible to change than the frequency of each rot type. Instead of pushing for a focus on one rot type over another, a prevalence of WR in temperate forests would support the need for future work that focuses on ecological traits that have enabled WR to dominate warmer forests and may enable them future dominance, relative to BR fungi, in warming boreal forests.

In our study, the most northern site, Marcell, was at the southern limit of the North American boreal forest zone but was not enriched in BR fungi contradicting our second prediction (P2). This might indicate that instead of a latitudinal continuum of WR/BR fungal dominance, the global distribution of these two wood-rotting fungal guilds might be associated with a latitudinal threshold separating WR- and BR-dominated areas. It is also important to note that a regional scale, Fukasawa et al. (2021) found that BR-fungi frequency was positively correlated with MAT, indicating that regional and continental drivers of the wood-rotting guilds occurrence might be different. Interestingly, SR fungi were the second most abundant wood-rotting fungal guild,

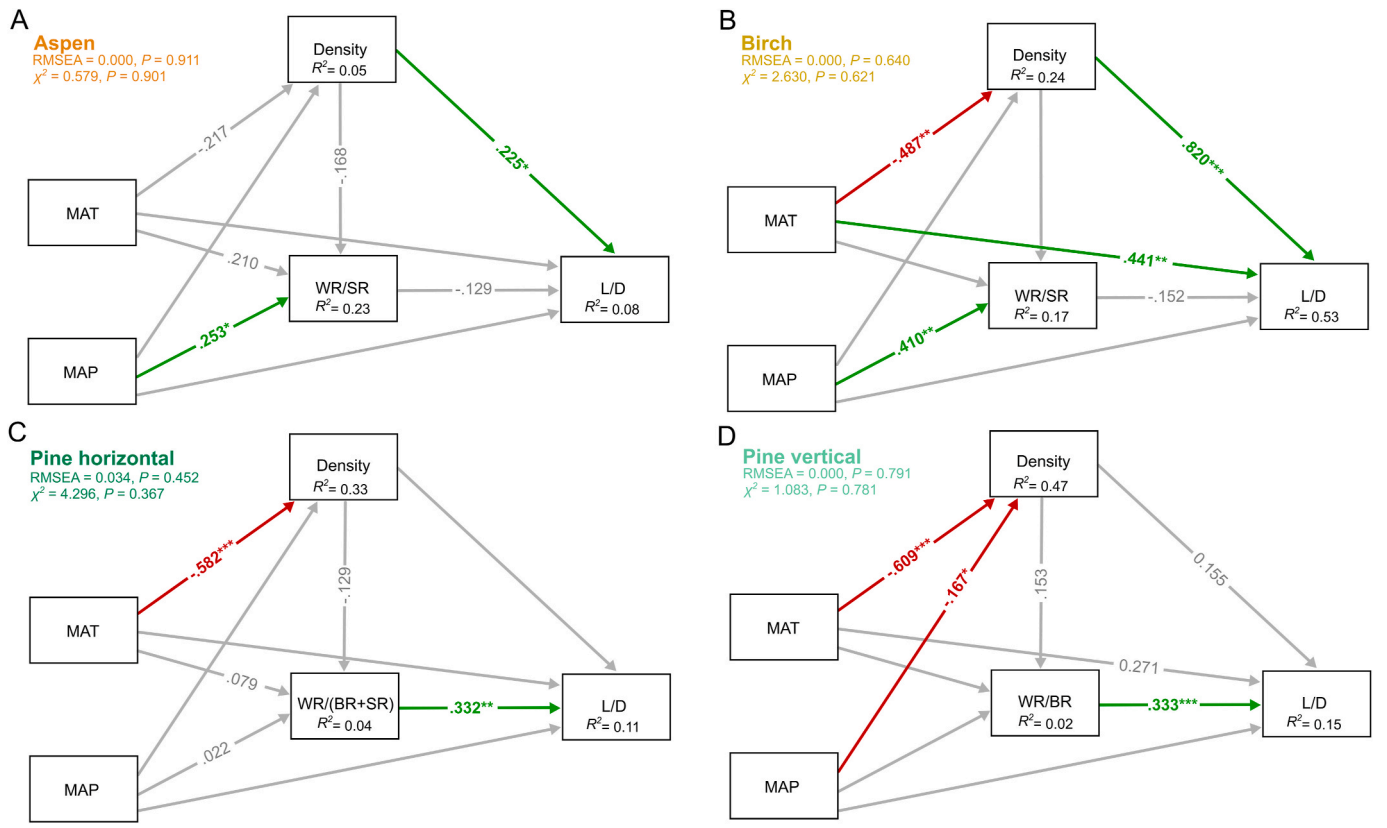

Fig. 5. Structural equation model (SEM) showing the effects of climate (MAP and MAT), wood density, and rot type relative abundance ratios on L/D for (A) aspen, (B) birch, (C) horizontal pine, and (D) vertical pine dead wood. Red and green colored arrows respectively represent significant negative and positive effects. The standardized path coefficient is indicated along with the arrows. The arrows lacking standardized path coefficients were not included in the SEM. The r^2 values represent the proportion of total variance explained for the dependent variable of interest. (For interpretation of the references to color in this figure legend, the reader is referred to the Web version of this article.)

reaching the same abundance as WR fungi for aspen and birch dead wood. Although it is hard to disentangle effects, it is possible that SR contributed to low L/D values that would normally be attributed to BR-dominated decay in a field study. Our SR fungal results are in agreement with most of the previous studies conducted in temperate forests (Arnstadt et al., 2016; Baldrian et al., 2016; Leonhardt et al., 2019) and contradict the narrative of SR fungi as organisms of extreme ecological niches (Blanchette et al., 2010). The importance of the geographic distribution of SR fungi might be underestimated in the literature due to the ambiguous trophic status of most members of this group. For example, some SR fungal species have a pathogenic and/or endophytic lifestyle, limiting their precise classification when the trophic status supersedes decay type during data analysis (Nguyen et al., 2016).

For the pine tree species, log orientation strongly affected wood-rotting fungal guilds by drastically increasing the relative abundance of BR fungi and decreasing the relative abundance of WR fungi. These observations parallel a recent study showing that BR fungi were more abundant in dead logs lacking ground contact (Jaroszewicz et al., 2021). The central hypothesis to explain this phenomenon is that dead logs standing vertically represent a less competitive habitat for BR fungi as compared to dead wood in contact with forest soil due to potentially limited colonization by soil fungi (Song et al., 2017). Because SR fungi also exhibited increased abundance in vertical dead wood in our study, we propose that competition between wood-rotting types mainly occurs between BR and WR fungi and not between BR and SR fungi. Priority effects experiments have already highlighted the potential lack of competitive abilities of BR fungi versus WR fungi. For example, Song et al. (2015, 2017) determined that when inoculated on sterilized dead birch wood in microcosms, BR fungal species were able to remain. Conversely, BR fungi were not able to colonize and persist on non-sterilized dead birch wood when incubated in the field (Cline et al., 2018). These observations might be associated with BR fungi life cycle because they have mostly been found as abundant in wood's early and mid-decay stages (Renvall, 1995; Rajala et al., 2012, 2015). The BR fungi could allocate more energy to rapid wood decomposition and sporocarp formation to colonize fresh dead wood or non-healthy living trees than compete with other fungi to defend territories or colonize new spaces. Taken together, our results suggest that dead wood standing vertically might represent a key ecological niche and a diversity reservoir for BR fungi in temperate forests.

The WR decay (L/D ratio) was the most frequently found wood-rotting type for the three studied tree species decomposing horizontally. However, on average, the L/D ratio was significantly lower for pine than for aspen and birch, which agrees with our third prediction (P3). It was possible to clearly distinguish two patterns in L/D ratio drivers between aspen/birch and pine. The L/D ratio implied a WR dominance for aspen and birch dead wood. Concerning the factors influencing wood decay type, for both aspen and birch, the L/D ratio was significantly positively correlated with wood density at the sampling time, often depicted as a proxy of the decomposition rate (Rajala et al., 2015). In other words, when the wood density is low, at the more advanced decay stages, the L/D ratio converged around 1.2–1.4, which corresponds with the maximum lignin removal by WR rot fungi at the end of decomposition (Schilling et al., 2015, 2020). Consequently, for aspen and birch, the L/D ratio is indirectly mediated by MAT (significantly for birch and as the trend for aspen) that accelerated wood decomposition (i.e. density at sampling in our study). Temperature control of wood decomposition rates has notably been described on a large scale and might result from an acceleration of the growth and activity of fungal decomposers

(Lustenhouwer et al., 2020).

MAT affected the decay rates (density at sampling) for pine dead wood, but the density was not associated with the L/D ratio. Dead wood decomposed by BR or SR fungi had values below 0.8, which is not associated with decomposition time, as we observed in this study with the lack of correlation between wood density and L/D ratio for pine dead wood (Schilling et al., 2020). The main factor influencing the L/D ratio was the ratio of WR to (BR + SR), suggesting that BR and SR fungi together were able to affect pine wood chemistry. These results contrast with aspen and birch wood. Despite being more abundant than in pine dead wood, SR fungi were statistically not associated with the L/D ratio, suggesting some BR and SR fungi cooperation during wood decomposition. Both MAT and MAP were associated with wood density at sampling for the vertical pine treatment, showing that moisture might be a limiting factor in the decomposition of vertically standing logs. The L/D ratio of vertical pine was similar to that of horizontal pine dead wood, which is not in agreement with our fourth prediction (P4) but, instead, was driven by the ratio between WR and BR fungi. Collectively, these pieces of evidence demonstrate that even if BR fungi were relatively poorly abundant and diverse, on average, they could affect the pine L/D strongly, whether alone or in association with the SR fungi.

How potential climatic parameters affect wood-rotting guild balance and L/D on a large scale remains relatively unknown (Fukasawa, 2021). MAP and MAT, respectively, influenced abundance and richness ratios of WR/SR without functional consequences to the L/D ratio for aspen or birch. Specifically, despite being as abundant as the WR fungi, the SR fungi colonizing aspen or birch had little influence on. We found a negative relationship between MAP and WR/(BR + SR) richness ratios for the vertical pine logs. Thus, a wetter climate could disadvantage WR fungi and/or favor BR and SR fungi leading to a potential increase of lignin-derived SOM. Finally, both of the wood-rotting fungal guild models using relative abundance and richness gave similar outputs concerning wood density and L/D, with a slight advantage in the abundance-based approach. However, richness-based models performed well in predicting the wood-rotting fungal guilds balance, notably for the horizontal logs. Consequently, both abundance- and richness-based wood-rotting fungi guild ratios represent promising predictive variables to integrate into forest soil carbon biogeochemical models.

While this study provides several new insights into the large-scale factors influencing wood decay types, important caveats should be considered. The choice of incubated wood originating from the same geographic region and then translocated across large-scale climatic gradients presents the advantage of a robust determination of the potential effects of climate parameters on wood decomposition processes. Nevertheless, in our study, some tree species were incubated out of the natural range of their distribution, which appears unrealistic regarding the climatic conditions dead wood of these species would encounter during their decomposition. Additionally, most of our study sites were dominated by gymnosperm trees, thus potentially limiting and/or biasing the fungal decomposer reservoirs. Consequently, depending on the specificity of the different fungal species for their woody substrates, we might have under- or over-estimated the abundance of some of the wood-rotting fungal guilds associated with aspen and birch dead wood. It is also important to note that all the boles initially came from the same forest sites in our transplant experiment. As such, the wood decomposition trajectories measured in our study might have been influenced by the community composition of the initial fungal pre-colonizers (i.e. wood endophytes) from the originating log sites (Song et al., 2017; Cline et al., 2018; Maillard et al., 2021). New studies investigating the factors influencing the wood-rotting fungal abundances at forest sites having adequate decomposer reservoirs will be important in validating the observed patterns. Finally, we did not capture the fungal successions because we sampled wood only once. This might explain the potential lack of correlations between the wood-rotting fungal guilds and the wood chemistry for aspen and birch, with L/D resulting from the successive waves of decomposers and fungal metabarcoding being a snapshot of the wood-inhabiting fungi at the sampling time.

5. Conclusion

Our study represents the first attempt to bridge wood-decay type and the different groups of wood-rotting fungi on a large spatial scale and using large-diameter tree boles. The results showed that WR fungi dominate the wood decomposition processes in temperate forests independently of the tree species or log position. SR fungi were much more abundant and diverse than expected, but without clear functional consequences on the L/D ratio for angiosperm tree species. Aspen and birch L/D ratios were best explained by warmer temperatures accelerating the decay rates and thus causing the diminution of L/D ratios. In contrast, BR fungi alone or in association with SR fungi were able to modify the L/D ratio for pine dead wood drastically. Across a large-scale log transplant experiment, we demonstrated that wood-rotting fungal guild balance governs the decomposition trajectories of dead wood. Thus, fungal decomposers are a source of organic matter physicochemical heterogeneity that is crucial to consider in modeling efforts for the long-term fate of C derived from woody material. Given the suspected opposite consequences of WR and BR/SR fungi on the fate of wood-derived C, even slight changes in the wood-rotting fungal guild balance due to forest management practices or climate change might have major impacts on the forest C cycle. Future studies are needed to improve predictions of the wood-rotting fungal abundance and diversity and their respective effects on the global C cycle.

Funding

The authors acknowledge support provided by the U.S. Department of Energy (16SC503106 to USDA Forest Service) and the National Science Foundation (DEB 1754603 to Michigan Technological University; DEB 1754616 to University of Minnesota). Funding also provided by the USDA Forest Service, Northern Research Station.

Declaration of competing interest

The authors declare no conflict of interests.

Acknowledgements

We would like to thank L. Boddy and two anonymous reviewers for their helpful comments and suggestions on previous versions of this manuscript. We thank the Caspar Creek, San Dimas, Sierra Ancha, Fraser, Tenderfoot Creek, Marcel, Coweeta, Santee Experimental Forests (USDA Forest Service) and the Duke Forest for hosting the FWDE. We appreciate the field crews led by Julie Arnold (Southern Research Station) and Joanne Tirocke (Rocky Mountain Research Station) for the sample collections and maintenance of the FWDE sites.

Appendix A. Supplementary data

Supplementary data to this article can be found online at https://doi.org/10.1016/j.funeco.2022.101151.

References

A'bear, A.D., Jones, T.H., Kandeler, E., Boddy, L., 2014. Interactive effects of temperature and soil moisture on fungal-mediated wood decomposition and extracellular enzyme activity. Soil Biol. Biochem. 70, 151–158.

Arnstadt, T., Hoppe, B., Kahl, T., Kellner, H., Krüger, D., Bauhus, J., et al., 2016. Dynamics of fungal community composition decomposition and resulting deadwood properties in logs of *Fagus sylvatica, Picea abies* and *Pinus sylvestris*. For. Ecol. Manag. 382, 129–142, 2016.

Baldrian, P., Lindahl, B., 2011. Decomposition in forest ecosystems: after decades of research still novel findings. Fungal Ecol. 4, 359–361.

Baldrian, P., Zrustova, P., Tlaskal, V., Davidova, A., Merhautova, V., Vrska, T., 2016. Fungi associated with decomposing deadwood in a natural beech-dominated forest. Fungal Ecol. 23, 109–122.
Blanchette, R.A., 1980. Wood decay—a sub-microscopic view. J. For. 78, 734–737.
Blanchette, R.A., Held, B.W., Arenz, B.E., Jurgens, J.A., Baltes, N.J., Duncan, S.M., et al., 2010. An antarctic hot spot for fungi at Shackleton's historic hut on cape royds. Microb. Ecol. 60, 29–38.
Bradford, M.A., Warren, R.J., Baldrian, P., Crowther, T.W., Maynard, D.S., Oldfield, E.E., Wieder, W.R., Wood, S.A., King, J.K., 2014. Climate fails to predict wood decomposition at regional scales. Nat. Clim. Change 4, 625–630.
Bugos, R.C., Sutherland, J.B., Adler, J.H., 1988. Phenolic compounds utilization by soft rot fungus Lecythophora hoffmanni. Appl. Environ. Microbiol. 54, 1882–1885.
Canadell, J.G., Raupach, M.R., 2008. Managing forests for climate change mitigation. Science 320, 1456–1457.
Chambers, J.Q., et al., 2000. Decomposition and carbon cycling of dead trees in tropical forests of the central Amazon. – Oecologia 122, 380–388.
Cline, L.C., Schilling, J.S., Menke, J., Groenhof, E., Kennedy, P.G., 2018. Ecological and functional effects of fungal endophytes on wood decomposition. Funct. Ecol. 32 (1), 181–191.
Dai, Z., Trettin, C.C., Burton, A.J., Jurgensen, M.F., Page-Dumroese, D.S., Forschler, B.T., et al., 2021. Coarse woody debris decomposition assessment tool: model validation and application. PLoS One 16 (7), e0254408.
Davidson, E.A., Janssens, I.A., 2006. Temperature sensitivity of soil carbon decomposition and feedbacks to climate change. Nature 440, 165–173.
Del Cerro, C., Erickson, E., Dong, T., Wong, A.R., Eder, E.K., Purvine, S.O., Mitchell, H.D., Weitz, K.K., Markillie, L.M., Burnet, M.C., et al., 2021. Intracellular pathways for lignin catabolism in white-rot fungi. Proc. Natl. Acad. Sci. U.S.A. 118, e2017381118.
Edenhofer, O., Pichs-Madruga, R., Sokona, Y., et al., 2014. Climate Change 2014: Mitigation of Climate Change. Contribution of Working Group III to the Fifth Assessment Report of the Intergovernmental Panel on Climate Change. Cambridge University Press, Cambridge, UK and New York, NY, USA.
Edgar, R.C., 2013. UPARSE: highly accurate OTU sequences from microbial amplicon reads. Nat. Methods 10, 996–998.
Edgar, R.C., Flyvbjerg, H., 2015. Error filtering, pair assembly and error correction for next-generation sequencing reads. Bioinformatics.
Eriksson, K-EL., Blanchette, R.A., Ander, P., 1990. Microbial andenzymatic degradation of wood and wood components. Springer, pp. 407–p.
Eslyn, W.E., Kirk, T.K., Effland, M.J., 1975. Changes in the Chemical Composition of Wood Caused by Six Soft-Rot Fungi Phytopathology, vol. 65, pp. 473–476.
Fierer, N., Grandy, A.S., Six, J., Paul, E.A., 2009. Searching for unifying principles in soilecology. Soil Biol. Biochem. 41, 2249–2256.
Frøslev, T.G., Kjøller, R., Bruun, H.H., Ejrnæs, R., Brunbjerg, A.K., Pietroni, C., Hansen, A. J., 2017. Algorithm for post-clustering curation of DNA amplicon data yields reliable biodiversity estimates. Nat. Commun. 8 (1), 1188.
Fukasawa, Y., 2015b. The geographical gradient of pine log decomposition in Japan. For. Ecol. Manag. 349, 29–35.
Fukasawa, Y., 2021. Ecological impacts of fungal wood decay types: a review of current knowledge and future research directions. Ecol. Res. https://doi.org/10.1111/1440-1703.12260.
Fukasawa, Y., Matsukura, K., 2021. Decay stages of wood and associated fungal communities characterise diversity-decomposition relationships. Sci. Rep. 11, 8972.
Fukasawa, Y., Matsuoka, S., 2015a. Communities of wood-inhabiting fungi in dead pine logs along a geographical gradient in Japan. Fungal Ecol. 18, 75–82.
Fukasawa, Y., Ando, Y., Oishi, Y., Matsukura, K., Okano, K., Song, Z., Sakuma, D., 2019. Effects of forest dieback on wood decay, saproxylic communities, and spruce seedling regeneration on coarse woody debris. Fungal Ecol. 41, 198–208.
Fukasawa, Y., et al., 2021. Relative importance of climate, vegetation, and spatial factors in the community and functional composition of wood-inhabiting fungi in discontinuously distributed subalpine spruce forests. Can. J. Res. 51.
Gilbertson, R.L., 1980. Wood-rotting fungi of North America. Mycologia 72 (1), 1–49.
Harmon, M.E., Franklin, J.F., Swanson, F.J., Sollins, P., Gregory, S.V., Lattin, J.D., Cummins, K.W., 1986. Ecology of coarse woody debris in temperate ecosystems. Adv. Ecol. Res. 15, 133–302.
Harmon, M.E., Fasth, B., Woodall, C.W., Sexton, J., 2013. Carbon concentration of standing and downed woody detritus: effects of tree taxa, decay class, position, and tissue type. For. Ecol. Manag. 291, 259–267.
Harmon, M.E., Fasth, B.G., Yatskov, M., Kastendick, D., Rock, J., Woodall, C.W., 2020. Release of coarse woody detritus – related carbon: a synthesis across forest biomes. Carbon Bal. Manag. 1–21.
Hoppe, B., Purahong, W., Wubet, T., Kahl, T., Bauhus, J., Arnstadt, T., et al., 2016. Linking molecular deadwood-inhabiting fungal diversity and community dynamics to ecosystem functions and processes in Central European forests. Fungal Divers. 77, 367–379.
Ihrmark, K., Bodeker, I.T.M., Cruz-Martinez, K., Friberg, H., Kubartova, A., Schenck, J., Strid, Y., Stenlid, J., Brandstrom-Durling, M., Clemmensen, K.E., et al., 2012. New primers to amplify the fungal ITS2 region – evaluation by 454- sequencing of artificial and natural communities. FEMS (Fed. Eur. Microbiol. Soc.) Microbiol. Ecol. 82, 666–677.
Jaroszewicz, B., Cholewinska, O., Checko, E., Wrzosek, M., 2021. Predictors of diversity of deadwood-dwelling macrofungi in a European natural forest. For. Ecol. Manag. 490, 119123.
Johnston, S.R., Boddy, L., Weightman, A.J., 2016. Bacteria in decomposing wood and their interactions with wood-decay fungi. FEMS Microbiol. Ecol. 92, 1–12.
Jusino, M.A., Skelton, J., Chen, C.C., Hulcr, J., Smith, M.E., 2020. Sexual reproduction and saprotrophic dominance by the ambrosial fungus flavodon subulatus (= flavodon ambrosius). Fungal Ecol. 47, 1–9.
Karunasekera, H., Daniel, G., 2015. Phylogenic, molecular and decay analysis of Phialophora species causing a soft rot of wood. Int. Wood Prod. J. 6, 189–197.
Keenan, T.F., Davidson, E.A., Munger, J.W., Richardson, A.D., 2013. Rate my data: quantifying the value of ecological data for the development of models of the terrestrial carbon cycle. Ecol. Appl. 23 (1), 273–286.
Krah, F.S., Bässler, C., Heibl, C., Soghigian, J., Schaefer, H., Hibbett, D.S., 2018. Evolutionary dynamics of host specialization in wood-decay fungi. BMC Evol. Biol. 18 (1), 119.
Leonhardt, S., Hoppe, B., Stengel, E., Noll, L., Moll, J., Bässler, C., Dahl, A., Buscot, F., Hofrichter, M., Kellner, H., 2019. Molecular fungal community and its decomposition activity in sapwood and heartwood of 13 temperate European tree species. PLoS One 14, e0212120.
Levy, J.F., 1969. The spectrum of interaction between fungi and wood. Rec. Ann. Conv. B.W.P.A. 71–78.
Lindner, D.L., Banik, M.T., 2011. Intragenomic variation in the ITS rDNA region obscures phylogenetic relationships and inflates estimates of operational taxonomic units in genus Laetiporus. Mycologia 103, 731–740.
Lindner, D.L., Vasaitis, R., Kubartova, A., Allmer, J., Johannesson, H., Banik, M.T., et al., 2011. Initial fungal colonizer affects mass loss and fungal community development in Picea abies logs 6 years after inoculation. Fungal Ecol. 4, 449–460.
Lustenhouwer, N., Maynard, D.S., Bradford, M.A., Lindner, D.L., Oberle, B., Zanne, A.E., Crowther, T.W., 2020. A trait-based understanding of wood decomposition by fungi. Proc. Natl. Acad. Sci. U.S.A. 117, 11551–11558.
Magnússon, R.I., Tietema, A., Cornelissen, J.H.C., Hefting, M.M., Kalbitz, K., 2016. Tamm Review: sequestration of carbon from coarse woody debris in forest soils. For. Ecol. Manag. 377, 1–15.
Maillard, F., Schilling, J., Andrews, E., Schreiner, K.M., Kennedy, P., 2020. Functional convergence in the decomposition of fungal necromass in soil and wood. FEMS (Fed. Eur. Microbiol. Soc.) Microbiol. Ecol. 96, fiz209.
Maillard, F., Andrews, E., Moran, M., et al., 2021. Early Chemical Changes during Wood Decomposition Are Controlled by Fungal Communities Inhabiting Stems at Treefall in a Tropical Dry Forest.
Mäkipää, R., Linkosalo, T., 2011. A non-destructive field method for measuring wood density of decaying logs. Silva Fenn. 45 (5).
Meinshausen, M., Meinshausen, H., Hare, W., Raper, S.B., Frieler, K., Knutti, R., Frame, D.J., Allen, M.R., 2009. Greenhouse gas emission targets for limiting global warming to 2°C. Nature 458, 1158–1163.
Nguyen, N.H., Song, Z., Bates, S.T., Branco, S., Tedersoo, L., Menken, J., Kennedy, P.G., 2016. FUNGuild: an open annotation tool for parsing fungal community datasets by ecological guild. Fungal Ecol. 20, 241–248.
Nilsson, T., 1973. Studies on wood degradation and cellulolytic activity of microfungi. Stud For Suec Nr 104.
Nilsson, T., Daniel, G., Kirk, T.K., Obst, J.R., 1989. Chemistry and microscopy of wood decay by some higher ascomycetes. Holzforschung 43, 11–18.
Oksanen, J., Blanchet, F.G., Friendly, M., Kindt, R., Legendre, P., McGlinn, D., Minchin, P.R., O'Hara, R.B., et al., 2013. Vegan: Community Ecology Package, R Package Version 2.5–6. 2019. Available: http://CRAN.R-project.org/package=vegan.
Palmer, J.P., Jusino, M.A., Banik, M.T., Lindner, D.L., 2018. Non-biological synthetic spike-in controls and the AMPtk software pipeline improve mycobiome data. PeerJ 6, e925.
Pedersen, N.B., Matthiesen, H., Blanchette, R.A., et al., 2020. Fungal attack on archaeological wooden artefacts in the Arctic—implications in a changing climate. Sci. Rep. 10, 14577.
Põlme, S., et al., 2020. FungalTraits: a user-friendly traits database of fungi and fungus-like stramenopiles. Fungal Divers. 105, 1–16.
Preston, C.M., Nault, J.R., Trofymow, J.A., 2009. Chemical changes during 6 years of decom-position of 11 litters in some Canadian forest sites. Part 2. 13C abundance, solid-state13C NMR spectroscopy and the meaning of"lignin. Ecosystems 12, 1078–1102.
R Core Team, 2021. R: A Language and Environment for Statistical Computing. R Foundation for Statistical Computing, Vienna, Austria. URL. http://www.R-project.org/.
Rajala, T., Peltoniemi, M., Pennanen, T., Mäkipää, R., 2012. Fungal community dynamics in relation to substrate quality of decaying Norway spruce (*Picea abies* [L.] Karst.) logs in boreal forests. FEMS Microbiol. Ecol. 81, 494–505.
Rajala, T., Tuomivirta, T., Pennanen, T., Mäkipää, R., 2015. Habitat models of wood-inhabiting fungi along a decay gradient of Norway spruce logs. Fungal Ecol. 18, 48–55.
Rayner, A.D.M., Boddy, L., 1988. Fungal communities in the decay of wood. Adv. Microb. Ecol. 10, 115–166.
Renvall, P., 1995. Community structure and dynamics of wood-rotting Basidiomycetes on decomposing conifer trunks in northern Finland. Karstenia 35, 1e51.
Riley, R., Salamov, A.A., Brown, D.W., Nagy, L.G., Floudas, D., Held, B.W., Levasseur, A., Lombard, V., Morin, E., Otillar, R., Lindquist, E.A., Sun, H., LaButti, K.M., Schmutz, J., Jabbour, D., Luo, H., Baker, S.E., Pisabarro, A.G., Walton, J.D., Blanchette, R.A., Henrissat, B., Martin, F., Cullen, D., Hibbett, D.S., Grigoriev, I.V., 2014. Extensive sampling of basidiomycete genomes demonstrates inadequacy of the white-rot/brown-rot paradigm for wood decay fungi. Proc. Natl. Acad. Sci. Unit. States Am. 111, 9923e9928.
Rosseel, Y., 2012. Lavaan: an R package for structural equation, 2012 Modeling 48 (2), 36. Epub 2012-05-24.
Russel, M.B., Fraver, S., Aakala, T., Gove, J.H., Woodall, C.W., D'Amato, A.W., Ducey, M. J., 2015. Quantifying carbon stores and decomposition in dead wood: a review. For. Ecol. Manag. 350, 107–128.

Ryan, M.E., Schreiner, K.M., Swenson, J.T., Gagne, J., Kennedy, P.G., 2020. Rapid changes in the chemical composition of degrading ectomycorrhizal fungal necromass. Fungal Ecol. 45, 100922.
Schilling, J.S., Kaffenberger, J.T., Liew, F.J., Song, Z., 2015. Signature wood modifications reveal decomposer community history. PLoS One 10, e0120679.
Schilling, J.S., Kaffenberger, J.T., Held, B.W., Ortiz, R., Blanchette, R.A., 2020. Using wood rot phenotypes to illuminate the "gray" among decomposer fungi. Front. Microbiol. 11, 1288.
Skelton, J., Jusino, M.A., Carlson, P.S., Smith, K., Banik, M.T., Lindner, D.L., Palmer, J. M., Hulcr, J., 2019. Relationships among wood-boring beetles, fungi, and the decomposition of forest biomass, 2019 Mol. Ecol. 28.
Song, Z., Vail, A., Sadowsky, M.J., Schilling, J.S., 2015. Influence of hyphal inoculum potential on the competitive success of fungi colonizing wood. Microb. Ecol. 69, 758–767.
Song, Z., Kennedy, P.G., Liew, F.J., Schilling, J.S., 2017. Fungal endophytes as priority colonizers initiating wood decomposition. Funct. Ecol. 31, 407–418.
Stutz, K.P., Dann, D., Wambsganss, J., Scherer-Lorenzen, M., Lang, F., 2017. Phenolic matter from deadwood can impact soil properties, 2017 Geoderma 288, 204–212.
Stutz, K., Kaiser, K., Wambsganss, J., Santos, F., Berhe, A.A., Lang, F., 2019. Lignin from white-rotted European beech deadwood and soil functions, 2019 Biogeochemistry 145, 81–105.
Thornton, P.K., Ericksen, P.J., Herrero, M., Challinor, A.J., 2014. Climate variability and vulnerability to climate change: a review. Glob. Change Biol. 20, 3313–3328.
Trettin, C.C., Burton, A., Jurgensen, M.F., Page-Dumroese, D.S., Dai, Z., Oren, R., Forschler, B., Schilling, J., Lindner, D., 2021. Wood Decomposition and its Role in the Forest Carbon Cycle: the FACE Wood Decomposition Experiment. U.S. Department of Agriculture Forest Service, Southern Research Station, Asheville, NC, p. 33. https://doi.org/10.2737/SRS-GTR-262. Gen. Tech. Rep. SRS-262.
van der Wal, A., Ottosson, E., de Boer, W., 2014. Neglected role of fungal community composition in explaining variation in wood decay rates. Ecology 96, 124–133.
Viotti, C., Bach, C., Maillard, F., Ziegler-Devin, I., Mieszkin, S., Buée, M., 2021. Sapwood and heartwood affect differentially bacterial and fungal community structure and successional dynamics during Quercus petraea decomposition. Environ. Microbiol.
Wallenstein, M.D., Haddix, M.L., Ayres, E., Steltzer, H., Magrini-Bair, K.A., Paul, E.A., 2013. Litter chemistry changes more rapidly when decomposed at home but converges during decomposition-transformation. Soil Biol. Biochem. 57, 311–319.
Weedon, J.T., Cornwell, W.K., Cornelissen, J.H.C., Zanne, A.E., Wirth, C., Coomes, D.A., 2009. Global meta-analysis of wood decomposition rates: a role for trait variation among tree species? Ecol. Lett. 12, 45–56.
Worrall, J.J., Anagnost, S.E., Zabel, R.A., 1997. Comparison of wood decay among diverse lignicolous fungi. Mycologia 89, 199–219.
Zabel, R.A., Wang, J.K., Anagnost, S.E., 1991. Soft-rot capabilities of the major microfungi isolated from Douglas-fir poles in the northeast. Wood Fiber Sci. 23, 220–237.
Zalamea, M., González, G., Ping, C.L., Michaelson, G., 2007. Soil organic matter dynamics under decaying wood in a subtropical wet forest: effect of tree species and decay stage. Plant Soil 296, 173–185.
Zanne, A.E., Oberle, B., Dunham, K.M., Milo, A.M., Walton, M.L., Young, D.F., 2015. A deteriorating state of affairs: how endogenous and exogenous factors determine plant decay rates. J. Ecol. 103, 1421–1431.
Zhang, J., Figueroa, M., Castaño, J.D., Silverstein, K., Schilling, J.S., 2019. Gene regulation shifts shed light on fungal adaptation in plant biomass decomposers. mBio 10 e2176-19.